geoconvention
Calgary • Canada • May 11-13 2026

Aeromagnetic Spectral Inversion for Geothermal Energy Exploration and its Implication to Lithium Prospecting: An Alberta Case Study

Chigozie C. Ikechukwu[1], Chima Justin Ezekiel[1,2]*

[1, 2]Department of Earth, Energy, and Environment, University of Calgary*

[2]School of Public Policy, University of Calgary

[1*] chigozie.ikechukwu@ucalgary.ca

Abstract

Despite Alberta's mature energy sector, a province-wide geothermal assessment that can also directly guide lithium-rich brine exploration has remained lacking. This study bridges this gap by applying large-scale spectral inversion to high-resolution aeromagnetic data (acquired by the Alberta Geological Survey) across Alberta. By utilizing 66 overlapping blocks (205 km × 205 km) to probe deeper than the thick sedimentary pile, we have established a more refined and integrated thermal baseline than previously available bottom hole temperature, allowing for the simultaneous identification of geothermal sweet spots and lithium-brine prospecting corridors, we performed centroid-based spectral inversion to map the magnetic basement and thermal structure. Results show that the depth to the top of magnetic sources averages 0.85 km, the centroid depth averages 10.15 km, and the Curie point depth averages 19.46 km. Corresponding thermal models yield an average geothermal gradient of 30.52 °C/km and an average surface heat flow of 76.31 mW m^{-2}. Spatial analysis identifies a high-potential exploration corridor, centered on blocks B28, B15, B22, and B21, where Curie depths are <15 km and heat flow exceeds 100 mW m^{-2}. Critically, these high-heat-flux zones could potentially represent direct lithium exploration targets, as they drive the hydrothermal processes that enrich deep brines with lithium. This work demonstrates that aeromagnetic spectral inversion provides a cost-effective geothermal assessment whose results are immediately applicable to lithium prospecting, offering a unified roadmap for resource evaluation where previous studies lacked a clear link between geothermal potential and critical mineral exploration. Ultimately, this integrated framework serves as a critical catalyst for Canada's 2030 and 2050 net-zero targets, de-risking the development of the 'dual-resource' projects essential for securing a domestic supply of battery minerals and sustainable baseload energy in the transition to a global clean energy economy.

KEYWORDS: Alberta, Geothermal Exploration, Lithium-Brine, Spectral Inversion, Curie Point Depth, Geothermal Gradient, Heat Flow, Western Canada Sedimentary Basin

1. Introduction

Despite Alberta's mature energy sector, a province-wide integrated geophysical framework for the simultaneous assessment of geothermal energy and lithium-brine potential has remained largely unexplored. This study utilizes large-scale spectral inversion of high-resolution aeromagnetic data to map the crustal thermal architecture of the Western Canada Sedimentary Basin (WCSB). By adapting established spectral analysis workflows, we determined the Curie Point Depth (CPD), geothermal gradient, and heat flow across 66 overlapping blocks. The results identify distinct high-value "sweet spots" characterized by shallow magnetic basements and elevated heat flow, providing a new baseline for targeted exploration of renewable geothermal energy and critical mineral resources.

2. Methodology

The methodology adopted for this study follows the standard spectral analysis of aeromagnetic data to estimate the depth to the bottom of magnetic sources, known as the Curie Point Depth (CPD)). The workflow assumes that at the CPD, dominant magnetic minerals (e.g., magnetite) transition from ferromagnetic to paramagnetic states at approximately 580 °C Bhattacharya and Leu,1975, Shuey et al. 1977, Blakely 1988, Afshar et al. 2016).

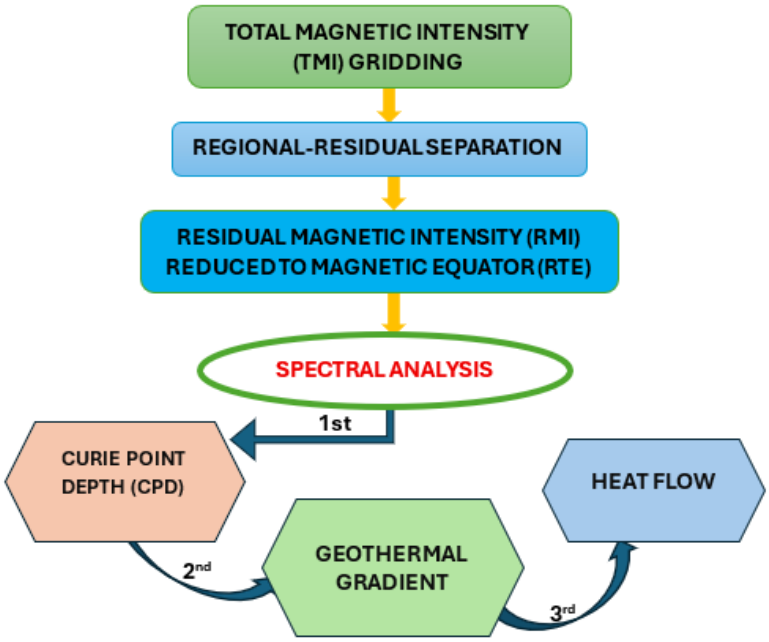


Figure 1: Methodology Flow Chart of Spectral Inversion of Aeromagnetic for Curie Point Depth, Geothermal Gradient, and Heat Flow.

The study area was divided into 66 overlapping blocks, each measuring 205 km by 205 km. This window size was selected to capture deep crustal features, adhering to the principle that window dimensions must differ from the target depth to resolve the deep magnetic basement (Ross et al. 2006, Bouligand et al. 2009). For each block, the radial power spectrum of the magnetic anomalies was calculated. Following the centroid method (Bhattacharyya & Leu, 1975; Okubo et al., 1985), the depth to the top of the magnetic source (Z_t) and the depth to the centroid (Z_c) were estimated from the slopes of the high-wavenumber and low-wavenumber portions of the power spectrum, respectively (Ikechukwu et al. 2025)

The basal depth of the magnetic source (Z_b), representing the CPD, was calculated using the relationship

$$\mathbf{Z_b = 2Z_c - Z_t} \quad .....(1)$$

Subsequently, the geothermal gradient (dT/dZ) and heat flow (q) were derived using the equations defined by Tanaka et al. (1999) and Okubo et al. (1985):

$$\mathbf{dT/dZ = 580 / Z_b} \quad .....(2)$$

$$\mathbf{q = k\,(dT/dZ)} \quad .....(3)$$

where 580 °C is the Curie temperature and is the thermal conductivity, measured to be the average thermal conductivity of the sampled crystalline basement rocks, with value of 2.5 W/m/°C.

3. Results and Discussions

The spectral inversion yielded a comprehensive thermal model of the study area. Statistical analysis of the inverted data reveals a depth to the top of magnetic sources (Z_t) ranging from 0.54 to 1.12 km, with an average of 0.85 km. The centroid depths (Z_c) range from 7.37 to 13.02 km, with an average of 10.15 km. Consequently, the calculated Curie Point Depths (Z_b) span from 13.79 km to 25.37 km, averaging 19.46 km.

The derived thermal parameters indicate a geothermal gradient of 22.86-42.05 °C/km (average 30.52 °C/km) and surface heat flow of 57.16-105.14 mW/m² (average 76.31 mW/m²).

Spatial analysis highlights a primary exploration corridor with exceptional geothermal potential. Notable "sweet spots" identified in the results table include:

• **Block 28:** Exhibits the highest heat flow of 105.14 mW/m² and a shallow CPD of 13.79 km.

• **Block 15:** Shows a heat flow of 104.04 mW/m² with a CPD of 13.94 km.

• **Block 22:** Displays a heat flow of 102.34 mW/m² and a CPD of 14.17 km.

• **Block 21:** Indicates a heat flow of 99.43 mW/m² with a CPD of 14.58 km.

These blocks represent zones of crustal thinning and high heat flux. The elevated temperatures in these zones likely drive hydro-geochemical processes and rock-water interactions essential for lithium enrichment in deep formation brines. The integration of these results suggests that the identified anomalies are priority targets for co-production strategies.

The Geothermal heat flow map of Alberta is shown in Figure 2 below. The legend/map shows the heat flow values range from 57.165 to 105.097 mW/m². These results are consistent with the regional assessments conducted by Grasby et al. (2012), who identified the Western Canada Sedimentary Basin (WCSB) as a primary target for geothermal exploration due to these elevated thermal signatures.

Specifically, the Northern and Central parts of Alberta record very high flow (76.903 – 105.097 mW/m²). This high-latitude thermal anomaly is supported by the work of Gray et al. (2012), who attributed such values to the combined effects of high radiogenic heat production within the Precambrian basement and the insulating "blanketing effect" of the thick sedimentary cover in those regions. Conversely, the south-western part of Alberta records lower heat flow values (57.165 – 76.902 mW/m²). This spatial trend aligns with the observations of Majorowicz et al. (2014), whose studies confirm a general increase in heat flow from the southwest toward the north and northeast.

The significance of these values regarding the viability of geothermal energy sites is summarized in Table 1. According to the criteria established in the literature for sedimentary basins, the values identified in this study categorize the province into three distinct potential zones:

Table 1: Geothermal Resource Viability based on Calculated Heat Flow

Heat Flow Range (mW/m^2)	Viability Classification	Potential Applications
57 – 70 (Southwestern AB)	Low to Moderate	Geo-exchange (heat pumps), greenhouse heating, and small-scale direct use.
71 – 85 (Central AB)	Medium-High	District heating, industrial process heat, and large-scale agricultural use.
86 – 105+ (Northern/NW AB)	High (Commercial)	Electricity Generation (via Organic Rankine Cycle), high-temperature industrial heat, and "Enhanced Geothermal Systems" (EGS).

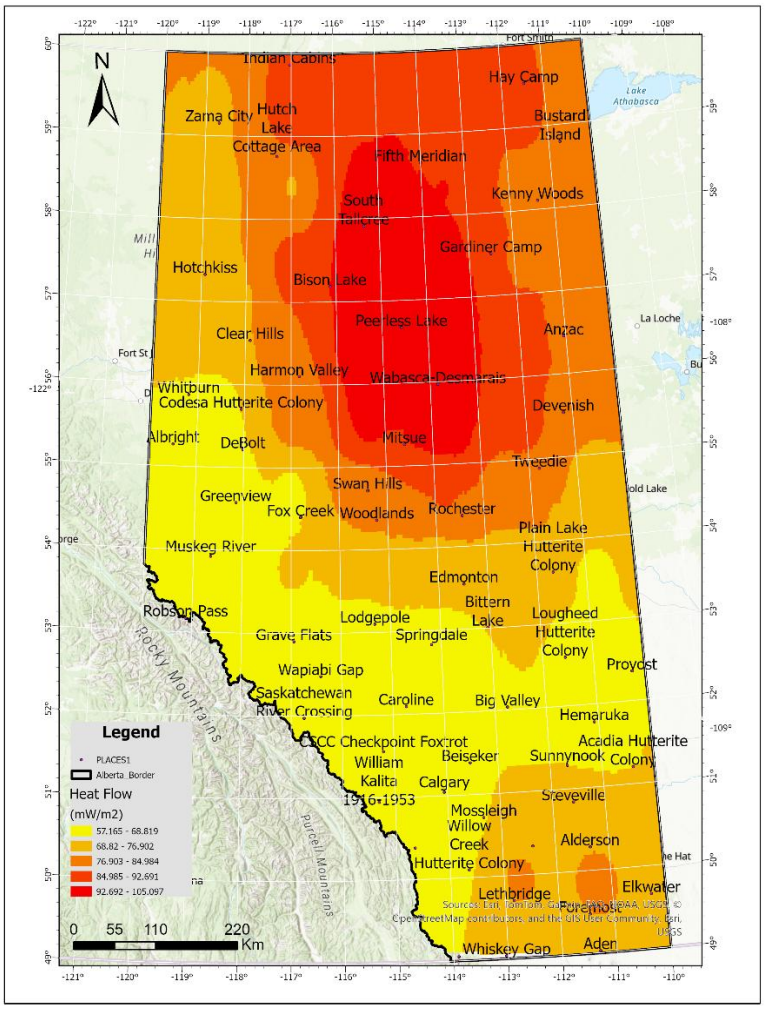


Figure 2: Alberta Heat Flow Map Derived from Spectral Inversion of Aeromagnetic Data

As noted by Majorowicz et al. (2014), the higher values observed in the Northern/NW regions are particularly critical, as they move the resource from simple direct-use applications into the viable range for commercial power generation. When compared to broader North American trends described by Blackwell et al. (2011), these northern Alberta values (>80 mW/m^2) rival many high-potential geothermal areas in the Western United States, such as the Basin and Range province. This indicates that Alberta's northern anomalies are not merely local curiosities but represent a significant continental-scale energy resource capable of supporting firm, carbon-neutral baseload power.

4. Novel Information

This research provides the first province-wide, high-resolution integration of aeromagnetic spectral inversion specifically tailored for dual geothermal and lithium-brine exploration in Alberta. Unlike previous studies that may have focused solely on hydrocarbon or singular geothermal metrics, this workflow identifies specific high-heat-flux corridors (e.g., Blocks 15, 21, 22, 28) as conductive environments for lithium enrichment. This approach offers a cost-effective, predictive roadmap for de-risking deep subsurface exploration.

5. Acknowledgements

We acknowledge the Alberta Geological Survey (AGS) for making the recently acquired aeromagnetic dataset publicly available. We also acknowledge the methodological foundations established by previous researchers in aeromagnetic spectral analysis.

References

Allan Gray, D., Majorowicz, J., & Unsworth, M. (2012). Investigation of the geothermal state of sedimentary basins using oil industry thermal data: case study from Northern Alberta exhibiting the need to systematically remove biased data. *Journal of Geophysics and Engineering*, *9*(5), 534-548.

Afshar, A., Norouzi, G. H., Moradzadeh, A., Riahi, M. A., & Porkhial, S. (2016). Curie point depth, geothermal gradient and heat-flow estimation and geothermal anomaly exploration from integrated analysis of aeromagnetic and gravity data on the Sabalan area, NW Iran. *Pure and Applied Geophysics*, *174*(3), 1133–1152.

Bhattacharyya, B. K., & Leu, L. K. (1975). Analysis of magnetic anomalies over Yellowstone National Park: Mapping of Curie point isothermal surface for geothermal reconnaissance. *Journal of Geophysical Research*, *80*(32), 4461–4465.

Blackwell, D., Richards, M., Frone, Z., Batir, J., Ruzo, A., Dingwall, R., & Williams, M. (2011). *Temperature-at-depth maps for the conterminous US and geothermal resource estimates* (No. GRC1029452). Southern methodist university geothermal laboratory, Dallas, TX (United States).

Blakely, R. J. (1988). Curie temperature isotherm analysis and tectonic implications of aeromagnetic data from Nevada. *Journal of Geophysical Research: Solid Earth*, *93*(B10), 11817-11832.

Bouligand, C., Glen, J. M., & Blakely, R. J. (2009). Mapping Curie temperature depth in the western United States with a fractal model for crustal magnetization. *Journal of Geophysical Research: Solid Earth*, *114*(B11).

Grasby, S. E., Jessop, A., Kelman, M., Ko, M., Chen, Z., Allen, D. M., ... & Therrien, R. (2011). Geothermal energy resource potential of Canada.

Ikechukwu, C. C., Opara, A. I., & Onyekuru, S. O. (2025). A review of various analytical techniques for estimating subsurface heat flow regimes from aero-geophysical data. *Arabian Journal of Geosciences*, *18*(6), 129.

Okubo, Y., Graf, R. J., Hansen, R. O., Ogawa, K., & Tsu, H. (1985). Curie point depths of the island of Kyushu and surrounding areas, Japan. *Geophysics*, *50*(3), 481–494.

Ross, H. E., Blakely, R. J., & Zoback, M. D. (2006). Testing the use of aeromagnetic data for the determination of Curie depth in California. *Geophysics*, *71*(5), L51-L59.

Shuey, R. T., Schellinger, D. K., Tripp, A. C., & Alley, L. B. (1977). Curie depth determination from aeromagnetic spectra. *Geophysical Journal International*, *50*(1), 75-101.

Spector, A., & Grant, F. S. (1970). Statistical models for interpreting aeromagnetic data. *Geophysics*, *35*(2), 293–302.

Tanaka, A., Okubo, Y., & Matsubayashi, O. (1999). Curie point depth based on spectrum analysis of the magnetic anomaly data in East and Southeast Asia. *Tectonophysics*, *306*(3), 461–470.

Weides, S., & Majorowicz, J. (2014). Implications of spatial variability in heat flow for geothermal resource evaluation in large foreland basins: the case of the Western Canada Sedimentary Basin. *Energies*, *7*(4), 2573-2594.